Mapping Structural Tensors from High-Resolution Trabecular Bone Images by 3D Spatial Autocorrelation

M. J. Wald[1], P. K. Saha[2], B. Vasilic[1], F. W. Wehrli[1]

[1]Laboratory for Structural NMR Imaging, University of Pennsylvania, Philadelphia, Pennsylvania, United States, [2]Medical Image Proecessing Group, University of Pennsylvania, Philadelphia, Pennsylvania, United States

Introduction:

The architecture of trabecular bone (TB), the sponge-like network found in the vertebrae and metaphysis and epiphysis of long bones, has been studied extensively as an indicator of bone quality and mechanical competence. TB is a quasi-periodic highly anisotropic network that remodels in response to the stresses to which it is subjected and it is known that osteoporosis increases the structural anisotropy (*1*). Further, the directions of structural anisotropy closely parallel the principal mechanical direction (*2*). Here, the three-dimensional spatial autocorrelation function (ACF) is introduced as a means to measure the anisotropic nature of TB thickness and spacing in high-resolution images. Specifically, the tensor computed from a 3D rose plot of the ACF is used to characterize the principal orientation and anisotropy of a TB network. The technique is validated by comparison to the fuzzy distance transform (FDT) (*3*) method and its robustness to noise using µCT and µMRI datasets.

Theory:

The continuous spatial autocorrelation function *ACF(x)* of a signal *f(x)* can be expressed by the two following formulas:

$$\text{(A)}\ ACF(x) = f(x) * f(x) = \int_{-\infty}^{\infty} f(x+x')\,f^{*}(x')dx' \qquad \text{(B)}\ ACF(x) = IFT\left(\left|FT(f(x))\right|^{2}\right)$$

where * represents the operation of convolution and *f*(x')* is the complex conjugate of *f(x')*. An efficient method of computing the ACF in 3D makes use of the Wiener-Khintchine theorem (B), which states that the ACF is equivalent to the inverse Fourier transform of the Fourier power spectral density.

Methods:

The 3D ACF is computed via (B) and then evenly sampled over a sphere by a given angular increment (3º) in spherical angular directions, θ and φ. Along each radial profile of the sphere, the full width at half maximum (FWHM) and the distance between consecutive maxima of the ACF are determined. These lengths represent the mean trabecular thickness and the mean trabecular spacing, respectively. The thickness data and the spacing data are then individually approximated by ellipsoids through minimization of the mean difference squared. The resulting ellipsoids or structural tensors, defined by three eigenvectors of magnitudes a, b, and c, render the orientational dependence of trabecular thickness and spacing within the 3-dimensional volume. The principal or major axes of both ellipsoids align with the direction of greatest TB thickness and largest spacing. Multiple measurements can be made by relating the orientation and magnitudes of the ellipsoidal axes. One such measurement is the anisotropy of the thickness and spacing and is determined by $(1\text{-}b^2/a^2)^{1/2}$, where 'a' is the length of the principal axis and 'b' is the length of the second largest axis. The ACF method was applied to twelve cylindrical samples (9mm x 9mm, cylinder axis parallel to radial shaft) from the human distal radius. Micro-CT images from eight specimens were obtained by µCT (N=8) and µMRI (N=4) at 16 and 78 µm isotropic resolution, respectively (µCT: MS-9, General Electric Medical Systems; MRI: 400 MHz, Bruker Instruments). To examine the effects of noise on the computation of thickness and spacing, Rician noise was added with varying amplitudes to a µCT dataset to mimic the noise properties of MR images. By varying the amplitude of the Gaussian noise distribution in frequency space, thickness and spacing measurements were calculated over a 25 :1 range in contrast-to-noise ratio (CNR).

Results:

Since the µCT samples are of higher resolution and represent larger datasets than the µMRI, results for the µCT are superior and were used to validate the ACF. Figure 1: A and B show cross-sectional planes of one of the 256^3 pixel µCT datasets in XY and XZ, respectively. Figure 1C is the XY plane of a typical µMRI dataset. Figures 2A and 2B show the sampled TB thickness and TB spacing data for a 3D µCT dataset, respectively, and the corresponding eigenvectors of the fit ellipsoids in red. All plane projections are shown for the thickness data in 2A while only the XY-plane-spacing-projection is shown in 2B. Note that the XY thickness projection in blue is isotropic while the XY spacing projection in green is anisotropic. Also, the largest red eigenvectors in both 2A and 2B are well correlated, an observation valid for all specimens.

Since the ACF is based on the bone signal versus the marrow-signal, it is more relevant to look at how the CNR between the two constituents affects the thickness and spacing measurements. Figure 4 shows how the ACF anisotropy in both thickness and spacing are affected by CNR levels. The anisotropy measurements begin to fail as the CNR approaches 3.

The means and standard deviations of anisotropy, offset angle, ACF and FDT measures for the eight µCT datasets are shown in Table 1. The offset angle is the angle between the principal axis of the ellipsoid and the longitudinal axis of the bone as it was cut from the radius. The ACF and FDT TB thickness and spacing measurements were analyzed using a paired T-test and found to be indistinguishable with p-values reported in Table 1.

Unlike the µCT images, the µMRI images needed to be cropped in order to remove the susceptibility artifacts arising from air bubbles within the sample. By removing the images with artifacts, the data size was reduced to 80x80x80 and the ACF was found to often fail in finding spacing values, i.e. second maxima, along the longitudinal direction (the general direction of largest thickness and spacing). The ellipsoids for the µMRI data were heavily weighted in the transverse plane and don't represent the overall anisotropic nature of the trabecular bone. While larger µMRI datasets are desirable, the ACF can still determine the mean TB thickness and TB spacing in the transverse plane. For the four µMRI sets, the mean thickness and spacing in the transverse plane are 161.8±10.2 and 940.3±69.5µm, respectively, which are within the expected ranges for TB thickness and spacing.

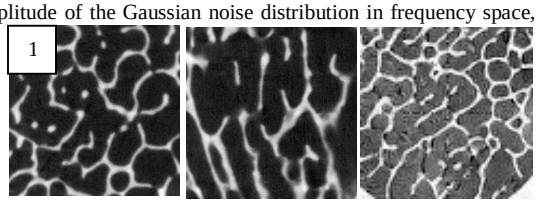

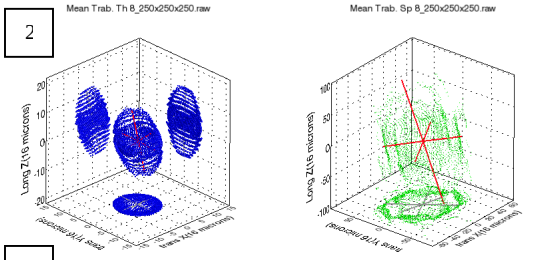

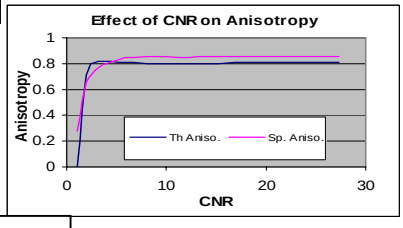

Table 1.

*p>0.05 is insignificant	Aniso.	ACF Offset θ º	ACF Results µm	FDT Results µm	Statistics
Sp. Mean	0.82	17.55	766.07	744.11	F=0.28
Stdev.	0.09	10.09	86.13	113.35	P=0.76*
Th. Mean	0.81	11.62	160.48	147.83	F=0.27
Stdev.	0.06	6.74	21.91	21.80	P=0.76*

Conclusions:

Trabecular bone can be locally described by the orientational dependence of its mean trabecular thickness and the mean trabecular spacing. The 3D spatial ACF is capable of determining the structural tensors of the trabecular thickness and spacing in both µCT and µMRI image sets of TB. The ACF is robust to noise and offers a simple method of analyzing the changing anisotropy of TB, which may provide a new metric for the study of osteoporotic bone loss and response to intervention.

References:

1. E. Ciarelli,D. P. Fyhrie,M. B. Schaffler,S. A. Goldstein, *J Bon. Miner Res.* **15**, 32-40 (2000).
2. A. Odgaard et al., *Journal of Biom. 3***0**, 487-495(1997).
3. P.K. Saha, F.W. Wehrli, *IEEE Trans. Med. Imag.* **30**, No.1, 53-62 (2004).

Acknowledgement: NIH Grant T32-EB000814